

## Supplementary Material

# A Synergistic Antibacterial Platform Combining Low-Temperature Photothermal Therapy and Antibiotic Therapy

Qiming Zhang <sup>1</sup>, Lei Chang <sup>2</sup>, Caixia Sun <sup>1</sup>, Wanchao Zuo <sup>1</sup>, Shibo Zhang <sup>1</sup>, Cong Liu <sup>1</sup>, Shuyue Deng <sup>1</sup>, Pengcheng Wu <sup>1</sup>, Panpan Dai <sup>1</sup>, Jianjun Dai <sup>1,3,4,\*</sup> and Yanmin Ju <sup>1,\*</sup>

<sup>1</sup> College of Pharmacy, China Pharmaceutical University, Nanjing 211198, China

<sup>2</sup> Department of Fundamental Research, Guangzhou Laboratory, Guangzhou 510005, China

<sup>3</sup> MOE Joint International Research Laboratory of Animal Health and Food Safety, College of Veterinary Medicine, Nanjing Agricultural University, Nanjing 210095, China

<sup>4</sup> Laboratory of Animal Bacteriology, Ministry of Agriculture, College of Veterinary Medicine, Nanjing Agricultural University, Nanjing 210095, China

\* Correspondence: jjdai@cpu.edu.cn (J.D.); juyanmin@cpu.edu.cn (Y.J.)

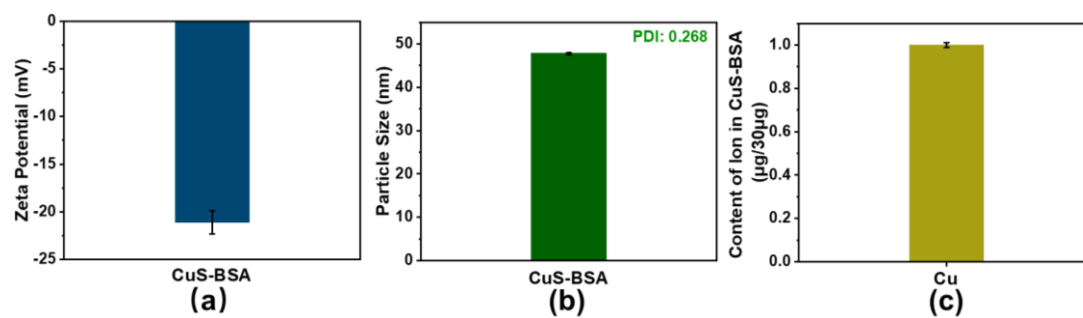


**Figure S1.** Characterization of CuS-BSA. (a) Zeta potential of CuS-BSA. (b) Particle size distribution of CuS-BSA in PBS. (c) Cu content in CuS-BSA.

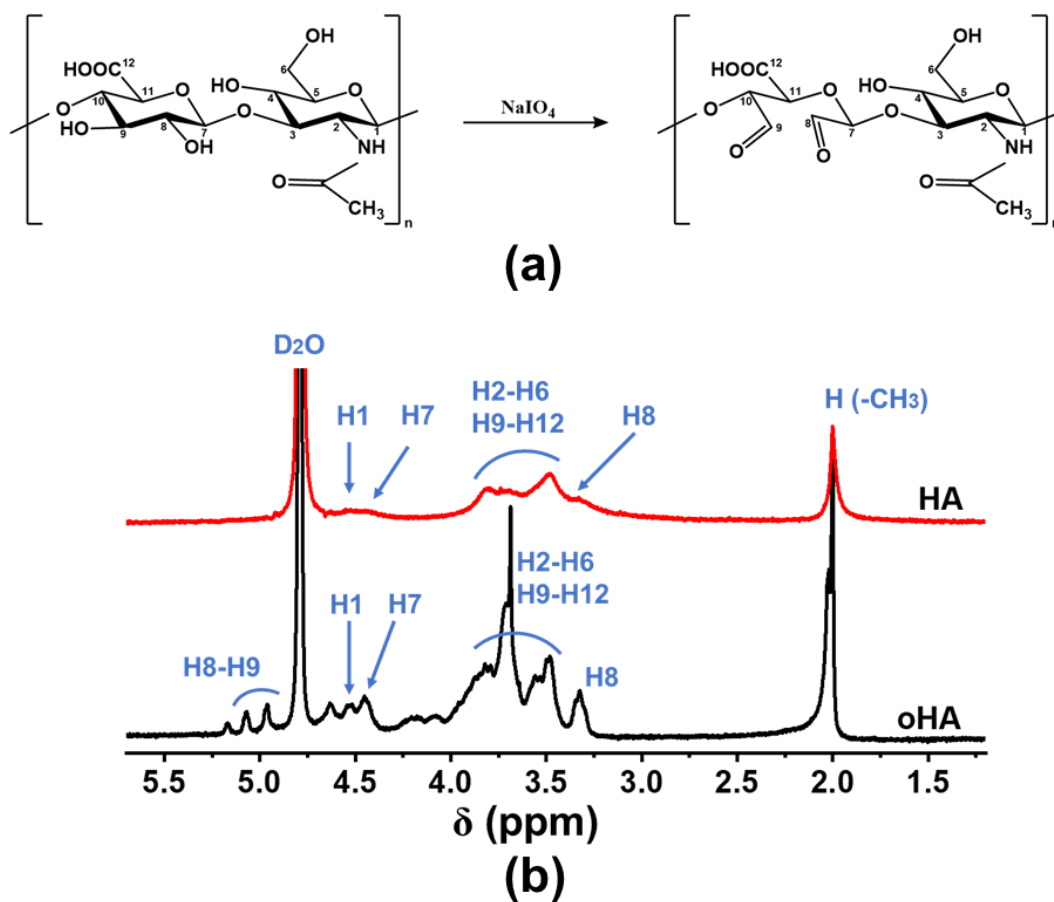


**Figure S2.** Characterization of oHA and HA. (a) Synthesis process of oHA. (b) NMR spectra and the corresponding peak assignment of oHA and HA.

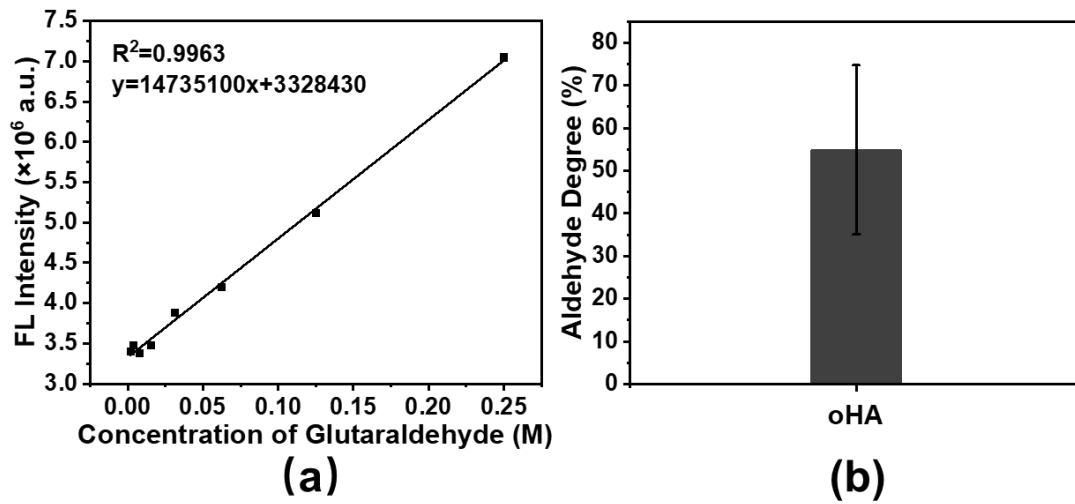


**Figure S3.** Calculation of aldehyde degree of oHA. **(a)** Linear regression curve of FL intensity with the concentration of glutaraldehyde. **(b)** Aldehyde degree of oHA.

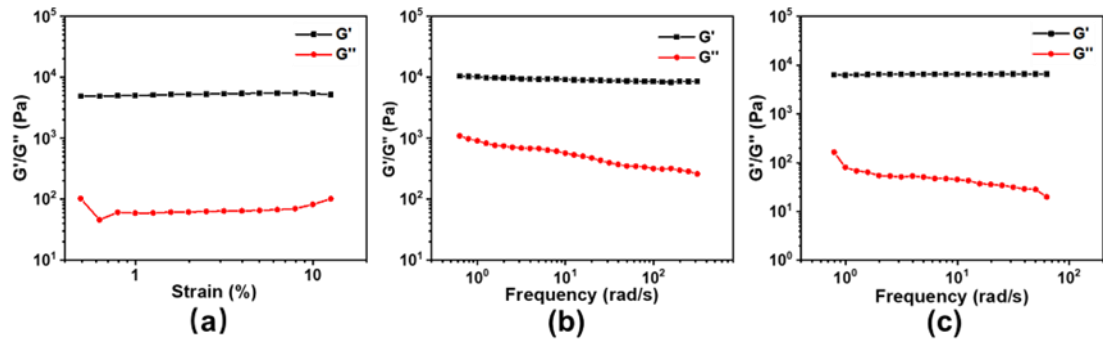


**Figure S4.** Rheological tests of Gel. (a) Plot of  $G'$  (elastic modulus) and  $G''$  (loss modulus) versus oscillation strain (0.5-12.5 %) at room temperature. (b) Plot of  $G'$  and  $G''$  versus frequency (1–300 rad/s) at 4 °C. (c) Plot of  $G'$  and  $G''$  versus frequency (1–60 rad/s) at 45 °C.

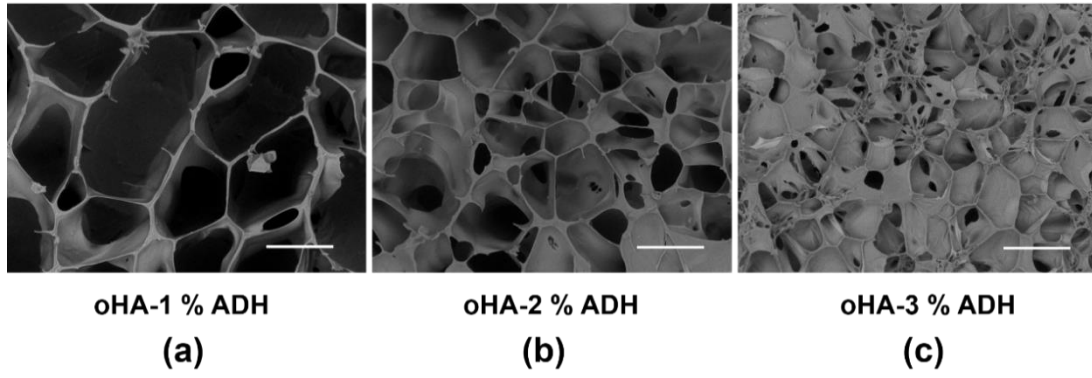


**Figure S5.** SEM images of Gel with different ADH concentrations of (a) 1 %, (b) 2 % and (c) 3 %, respectively. Scale bar: 100  $\mu\text{m}$ .

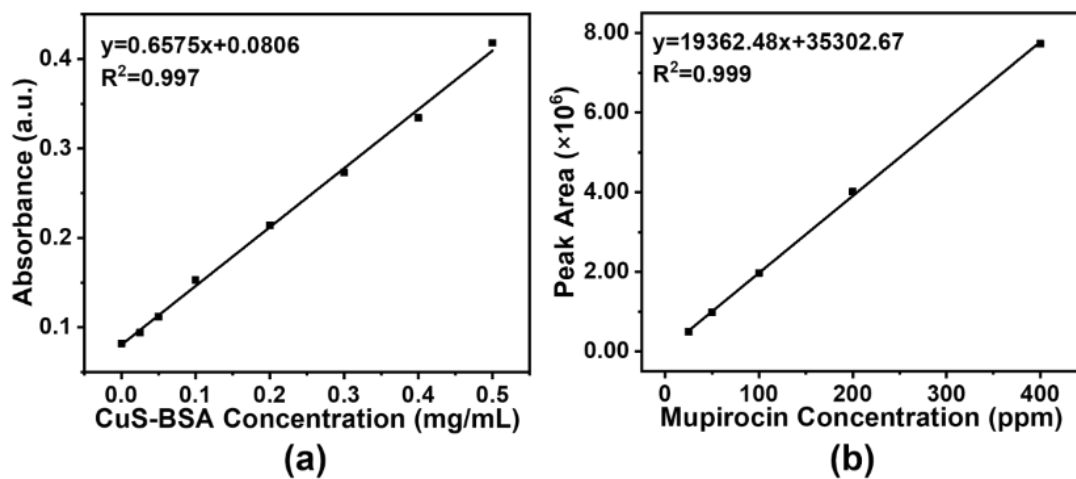


**Figure S6.** Standard curve of CuS-BSA and mupirocin. (a) Calibration curve of UV-vis absorbance versus different CuS-BSA concentrations of 0, 0.025, 0.05, 0.1, 0.2, 0.3, 0.4 and 0.5 mg/mL, respectively. (b) Calibration curve of peak area versus different mupirocin concentrations of 25, 50, 100, 200 and 400 ppm, respectively.

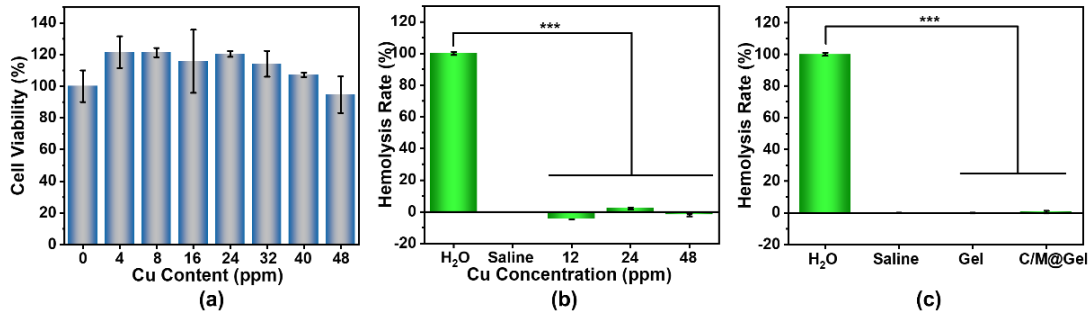


**Figure S7.** Biocompatibility of CuS-BSA and C/M@Gel. (a) Cell viability of CuS-BSA with different Cu concentrations of 0, 4, 8, 16, 24, 32, 40 and 48 ppm, respectively. (b) Hemolysis rates of RBCs after different treatments of H<sub>2</sub>O, saline and CuS-BSA with different Cu concentration of 12, 24 and 48 ppm, respectively. (c) Hemolysis rates of RBCs after different treatments of H<sub>2</sub>O, saline, Gel and C/M@Gel. (Error bar: mean  $\pm$  SD, \*\*\*P < 0.001).

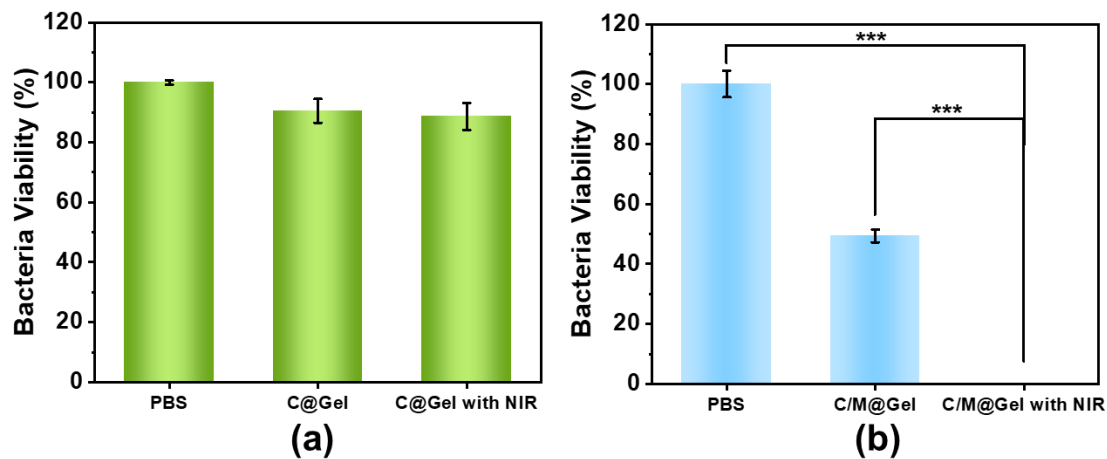


**Figure S8.** Comparison of bacteria viability in different groups with or without NIR irradiation. **(a)** The survival percentage of bacteria after incubating with PBS, C@Gel and C@Gel with NIR. **(b)** The survival percentage of bacteria after incubating with PBS, C/M@Gel and C/M@Gel with NIR. NIR irradiation time: 5 min, mupirocin concentration in C/M@Gel: 0.125 ppm, Cu concentration in C@Gel and C/M@Gel: 24 ppm. (Error bar: mean  $\pm$  SD, \*\*\*P < 0.001).

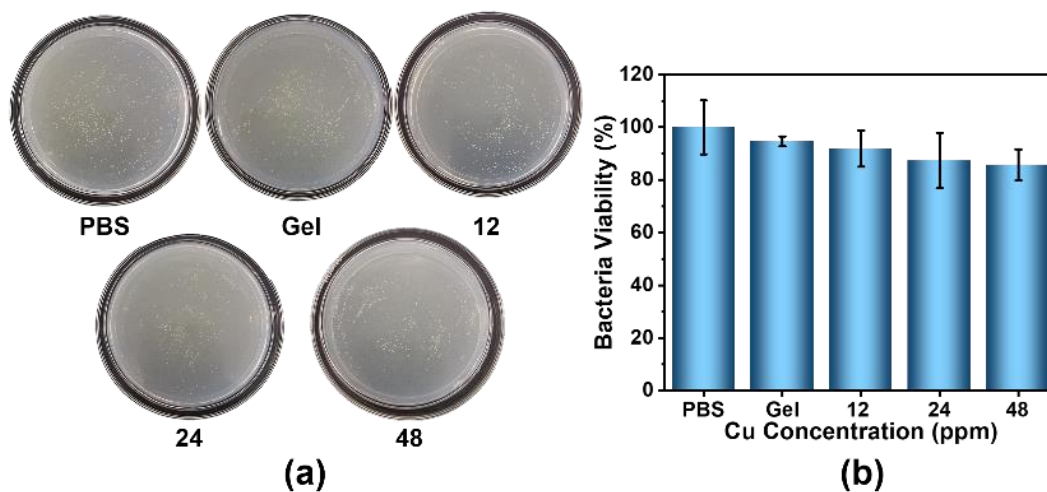


**Figure S9.** Antibacterial efficacy of C@Gel *in vitro*. **(a)** The results of standard plate counting and **(b)** the corresponding survival percentage of bacteria after incubating with PBS, Gel and C@Gel with different Cu concentrations of 12, 24 and 48 ppm, respectively.

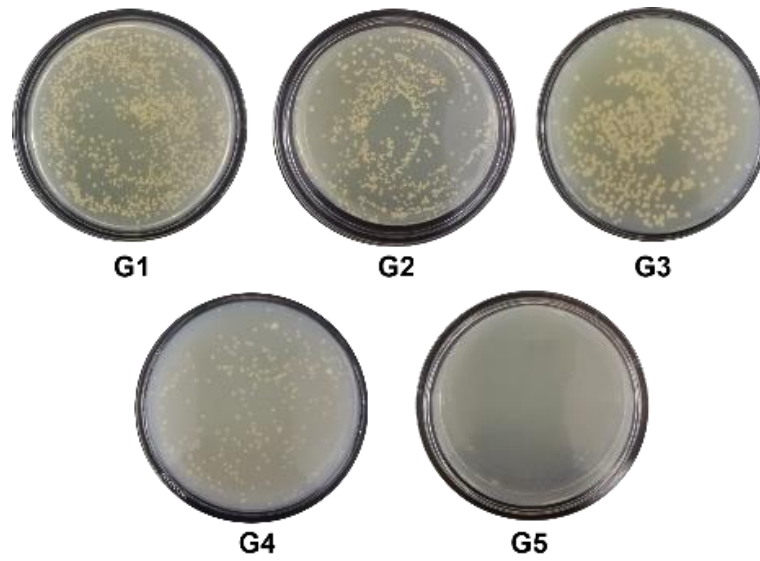


**Figure S10.** Standard plate counting of residual bacteria at the wound site after four consecutive days of mono/synergistic therapy. G1: PBS, G2: Gel, G3: C@Gel+NIR, G4: M@Gel, G5: C/M@Gel+NIR. Mupirocin concentration in M@Gel and C/M@Gel: 0.125 ppm, Cu concentration in C@Gel and C/M@Gel: 24 ppm.